

C-DGPA: Class-Centric Dual-Alignment Generative Prompt Adaptation

Chao Li¹, Dasha Hu^{1*}, Chengyang Li¹, Yuming Jiang¹, Yuncheng Shen²

¹ College of Computer Science, Sichuan University, Chengdu, China

² College of Physics and Information Engineering, Zhaotong University, Zhaotong, China

Abstract

Unsupervised Domain Adaptation transfers knowledge from a labeled source domain to an unlabeled target domain. Directly deploying Vision-Language Models (VLMs) with prompt tuning in downstream UDA tasks faces the significant challenge of mitigating domain discrepancies. Existing prompt-tuning strategies primarily align marginal distribution, but neglect conditional distribution discrepancies, leading to critical issues such as class prototype misalignment and degraded semantic discriminability. To address these limitations, the work proposes C-DGPA: Class-Centric Dual-Alignment Generative Prompt Adaptation. C-DGPA synergistically optimizes marginal distribution alignment and conditional distribution alignment through a novel dual-branch architecture. The marginal distribution alignment branch employs a dynamic adversarial training framework to bridge marginal distribution discrepancies. Simultaneously, the conditional distribution alignment branch introduces a Class Mapping Mechanism (CMM) to align conditional distribution discrepancies by standardizing semantic prompt understanding and preventing source domain over-reliance. This dual alignment strategy effectively integrates domain knowledge into prompt learning via synergistic optimization, ensuring domain-invariant and semantically discriminative representations. Extensive experiments on OfficeHome, Office31, and VisDA-2017 validate the superiority of C-DGPA. It achieves new state-of-the-art results on all benchmarks.

Code —

<https://anonymous.4open.science/r/C-DGPA-B37F>

Instruction

Unsupervised Domain Adaptation (UDA) transfers knowledge from a labeled source domain to an unlabeled target domain to enhance learning effectiveness. The core challenge lies in reducing distribution discrepancies between domains to improve model generalization on unlabeled target data without sacrificing semantic discriminability(Wilson and Cook 2020; Zhu et al. 2023a). Traditional UDA methods rely on adversarial training(Ganin and Lempitsky 2015) and metric learning(Saito et al. 2018; Tang, Chen, and Jia 2020; Zhang, Wang, and Gai 2020) to narrow distribution gaps

and achieve domain alignment. Although partially effective, these methods often incur semantic information loss and fail to disentangle domain knowledge from semantic content effectively(Zhang, Huang, and Wang 2022; Tang, Chen, and Jia 2020).

Concurrently, large-scale visual language models (VLMs), particularly CLIP(Radford et al. 2021), exhibit remarkable performance in UDA tasks due to their strong image-text integration capabilities(Hu et al. 2024; Lai et al. 2024). VLMs map visual and textual representations into a shared embedding space, reducing domain differences, and improving discriminative performance. Prompt tuning has emerged as an effective strategy for adapting VLMs to downstream unlabeled data. State-of-the-art techniques like CoOp(Zhou et al. 2022b) and MaPLe(Khattak et al. 2023) deliver strong performance on specific tasks: CoOp learns soft text prompts, while MaPLe employs visual-linguistic prompts to enhance interaction. Despite mitigating domain discrepancies, these techniques focus primarily on aligning marginal probability distribution through prompt, overlooking cross-domain conditional distribution discrepancies. This oversight causes:

- Class Prototype Shift(Tang, Chen, and Jia 2020) : Feature space misalignment between source and target domain prototypes (distribution centers) for the same class.

- Semantic Discriminability Degradation: Blurred class boundaries persist even after global feature alignment, leading to target sample misclassification.

Long(Long et al. 2015) demonstrated that the total domain discrepancy decomposes into the sum of marginal and conditional distribution discrepancies. Consequently, conditional alignment can significantly improve prompt performance against domain discrepancies, enabling deeper understanding and adaptation to diverse data distributions.

Inspired by Long et al, the work proposes C-DGPA (Class-Centric Dual-Alignment Generative Prompt Adaptation), the first class-centric dual-alignment method for generative prompt adaptation. C-DGPA employs dual branches (marginal distribution and conditional distribution alignment branch) to address limitations in cross-domain learning. The Marginal Distribution Alignment Branch employs adversarial training to minimize marginal distribution discrepancies, generating domain-invariant features through a dynamic minimax optimization framework with Gradient

*Corresponding author.

Copyright © 2026, Association for the Advancement of Artificial Intelligence (www.aaai.org). All rights reserved.

Reversal Layer (GRL). Meanwhile, the Conditional Distribution Alignment Branch addresses conditional distribution discrepancies via the proposed Class Mapping Mechanism (CMM), which standardizes semantic prompt representations for specific classes by aligning cross-domain class prototypes. This dual-branch architecture synergistically optimizes prompt parameters: the Marginal Distribution Alignment Branch ensures feature invariance across domains, while the Conditional Distribution Alignment Branch mitigates source domain over-reliance and enhances target domain discriminability by refining class-sensitive semantics. Key innovations include:

- The work proposes C-DGPA, a novel Class-Centric Dual-Alignment framework for generative prompt adaptation in UDA. C-DGPA is the first to integrate the Marginal Alignment Distribution Branch and Conditional Distribution Alignment Branch within a unified prompt tuning paradigm via synergistic dual-branch optimization.
- The work develops a dynamic adversarial alignment framework within the Marginal Distribution Alignment Branch. This framework, incorporating a minimax objective and a GRL, effectively aligns the marginal distribution across domains, generating domain-invariant prompt features crucial for subsequent class alignment.
- The work introduces the CMM as the core of the Conditional Distribution Alignment Branch. CMM explicitly addresses the critical challenge of conditional distribution discrepancies by mapping prompt features to a domain-invariant class prototype space, supervised by the conditional alignment loss. This mechanism is key to mitigating class prototype shift and enhancing semantic discriminability.

Our research findings show that C-DGPA performs excellently on benchmark datasets, including OfficeHome, Office31, and VisDA-2017. Compared with existing state-of-the-art methods, C-DGPA achieves significant performance improvements, proving its effectiveness in unsupervised domain adaptation tasks.

Related Work

Unsupervised Domain Adaptation

The core objective of UDA is to learn domain-invariant features by aligning distributions across domains. Early methods rely on statistical metrics such as maximum mean discrepancy (MMD)(Long et al. 2015) to minimize feature distribution gaps. Adversarial learning further advanced UDA by training domain-invariant features through minimax optimization. Domain-Adversarial Neural Networks (DANN)(Ganin et al. 2016) introduced gradient reversal layers to align domains, while Smooth Domain-Adversarial Training (SDAT)(Rangwani et al. 2022) improved generalization by smoothing source loss.

Vision-Language Models (VLMs)

Large-scale VLMs like CLIP(Hu et al. 2024; Lai et al. 2024) enable cross-modal alignment through contrastive pre-training, offering strong zero-shot transferability. To adapt VLMs to downstream tasks, prompt tuning has

emerged as a key paradigm. CoOp replaced manual prompts with learnable vectors, and MaPLe extended this to multimodal prompts. PDA(Bai et al. 2024) introduced dual-branch alignment for further marginal alignment distributions. However, existing methods primarily align marginal distributions, neglecting conditional distribution discrepancies. C-DGPA addresses these gaps by integrating a dynamic adversarial alignment framework for marginal distribution with CMM for conditional distribution.

Visual prompt tuning

By optimizing the input prompt vectors, the model can better understand and execute specific tasks. This approach is particularly prominent in few-shot(Gu et al. 2021) and zero-shot(Reynolds and McDonell 2021) learning environments. In recent years, researchers have proposed Visual Prompt Tuning (VPT)(Jia et al. 2022; Zhu et al. 2023b; Pfeiffer et al. 2023), which applies prompts to the visual domain. The core idea of prompting is to embed new prompt vectors for parameter training on the basis of the original model, while freezing the parameters of the original model. This allows the model to update only the parameters of the prompt during training, thereby achieving the desired optimization effect.

Preliminaries

Unsupervised Domain Adaptation

Unsupervised Domain Adaptation (UDA) focuses on transferring knowledge from a labeled source domain to an unlabeled target domain. The source domain C_s comprises a feature space x_s and a marginal distribution $P_s(x_s)$, while the target domain C_t consists of a feature space x_t and a marginal distribution $P_t(x_t)$. In the source domain, there is a sample set $x_s = \{x_1^s, x_2^s, \dots, x_N^s\}$ with corresponding labels $y_s = \{y_1^s, y_2^s, \dots, y_N^s\}$. In contrast, the target domain only contains a sample set $x_t = \{x_1^t, x_2^t, \dots, x_M^t\}$, where N and M represent the number of samples in the source and target domains, respectively. A model trained on the source domain is intended for testing on the target domain. However, in many application scenarios, such as face recognition, various factors(e.g., lighting, angles, expressions) can affect the target domain's data distribution. UDA addresses these challenges by mitigating the impact of such factors and enabling effective knowledge transfer from the labeled source domain to the unlabeled target domain.

Contrastive Language-Image Pretraining

CLIP (Contrastive Language-Image Pretraining) is a model capable of jointly processing images and text. It learns the relationship between images and text through pretraining. In downstream tasks, the pretrained CLIP model is adapted to specific tasks via manually designed prompts. The matching score between an image and text is calculated based on the cosine similarity $\langle \hat{w}_i, z \rangle$ between the image representation z and the text representation corresponding to the i -th class. The image representation is obtained by processing the input image with an image encoder, while the text representation is extracted from a text encoder using a prompt description

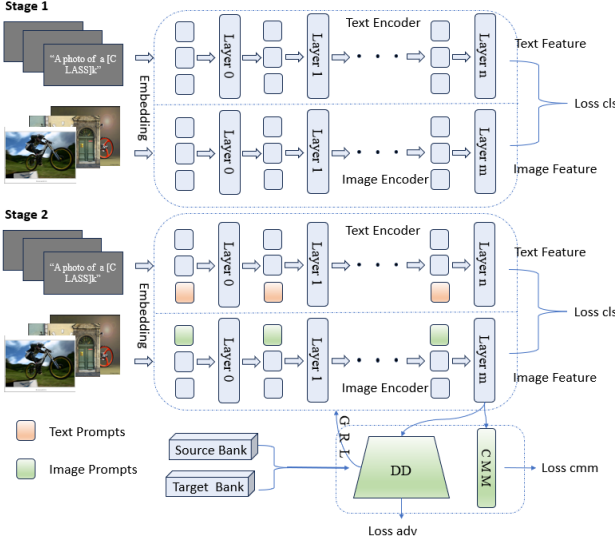


Figure 1: The architecture of the C-DGPA model. This figure illustrates the structure of our model at different stages. The Source Bank and Target Bank represent the feature banks of the source and target domains, respectively. CMM is used to map the image features I to the class space, while DD denotes the domain discriminator that generates domain labels based on I . In Stage 2, the blue color indicates the frozen parts, while other colors indicate the parts that need to be trained.

associated with the i -th class. The probability that an image belongs to the i -th class is given by:

$$P(y = i|x) = \frac{\exp(\langle \hat{w}_i, z \rangle / \tau)}{\sum_{j=1}^K \exp(\langle \hat{w}_j, z \rangle / \tau)} \quad (1)$$

Feature Bank Construction

Confidence scores are generated for source domain images. Target domain pseudo-labels are then determined. Subsequently, the top C features per class from both domains form a K -class feature bank (C per class). Class center features establish the source bank $f_s \in \mathbb{R}^d$ and target bank $f_t \in \mathbb{R}^d$. This ensures feature bank robustness and significantly improves cross-domain learning performance.

Theoretical Foundation for Dual-Alignment

Unsupervised Domain Adaptation aims to minimize the total domain discrepancies d_J between source and target distributions. As formalized by Long (Long et al. 2015), the distributions decompose into the sum of marginal distribution discrepancies $\bar{d}_H(P_s(x_s), P_t(x_t))$ and conditional distribution discrepancies $d_C(P_s(y_s|x_s), P_t(\hat{y}_t|x_t))$:

$$d_J(P_s, P_t) = d_H(P_s, P_t) + d_C(P_s, P_t) \quad (2)$$

$$d_C(P_s, P_t) = \mathbb{E}[\|\mathbb{P}(y_s|x_s) - \mathbb{P}(\hat{y}_t|x_t)\|] \quad (3)$$

Here, \hat{y}_t denotes the pseudo-labels generated for the target domain (Lai et al. 2023; Litrico, Del Bue, and Moreiro 2023).

Critically, the Ben-David theorem (Ben-David et al. 2010) establishes that the target domain error $\epsilon_T(p)$ is bounded by

$$\epsilon_T(p) \leq \epsilon_S(p) + d_J(P_s, P_t) + \lambda \quad (4)$$

where λ represents the optimal joint error. This theoretical decomposition necessitates a dual-alignment strategy:

- Marginal Distribution Alignment Branch resolves marginal distribution discrepancies

$$d_H(P_s(x_s), P_t(x_t)) \rightarrow 0 \quad (5)$$

- Conditional Distribution Alignment Branch resolves conditional distribution discrepancies

$$d_C(P_s(y_s|x_s), P_t(\hat{y}_t|x_t)) \rightarrow 0 \quad (6)$$

Where x denotes input images, and later alignment is performed on prompt-generated features $I = f(x; \theta_p)$. Therefore, our proposed dual-branch architecture is explicitly designed to minimize both terms concurrently: The Marginal Distribution Alignment Branch reduces marginal distribution discrepancies $d_H(P_s(I_s), P_t(I_t))$ via a Dynamic Adversarial Alignment Framework. The Conditional Distribution Alignment Branch minimizes conditional discrepancies $d_C(P_s(y_s|I_s), P_t(\hat{y}_t|I_t))$ through the CMM by projecting I into a semantically invariant space. By synergistically optimizing both objectives, C-DGPA directly suppresses $d_J(P_s, P_t)$, hereby lowering the upper bound of $\epsilon_T(p)$ —a theoretical advance unrealized by prior prompt-based UDA methods.

Method

The architecture of the original CLIP model is depicted in Stage 1 of Figure 1. In this setup, the text encoder produces text features $T = \{T_1, T_2, \dots, T_n\}$, while the image encoder generates image features $I = \{I_1, I_2, \dots, I_n\}$. C-DGPA employs a synergistic dual-branch architecture to achieve comprehensive domain adaptation through joint optimization of marginal and conditional distribution alignment (Long et al. 2015). As illustrated in Figure 1(Stage 2), the image features I generated by the prompt are processed concurrently by two distinct branches: The Marginal Distribution Alignment Branch: Implements our Dynamic Adversarial Alignment Framework to minimize marginal distribution discrepancy via adversarial training; The Conditional Distribution Alignment Branch: Leverages the Class Mapping Mechanism (CMM) to minimize conditional distribution discrepancies. The prompt parameters θ_p are jointly optimized by the combined loss $\mathcal{L} = \mathcal{L}_{cls} + \gamma_{cal}\mathcal{L}_{cal} + \gamma_{mal}\mathcal{L}_{mal}$, enabling the prompt to progressively learn both domain-invariant and class-discriminative representations. After fine-tuning the dual branches can be discarded, resulting in a lightweight adapted model. The symbols and their corresponding meanings used in this paper are presented in Table 1.

Marginal Distribution Alignment Branch: Dynamic Adversarial Alignment for Marginal Distribution

The primary objective of this branch is to align the marginal distribution $P_s(I_s) \approx P_t(I_t)$ by suppressing domain-

Symbol	Description	Symbol	Description	Symbol	Description
C_s, C_t	Source/target domain space	x_s, x_t	Source/target sample set	y_s	Source labels
L_{adv}	Marginal alignment loss	I_s, I_t	Source/target image features	\mathbb{R}^d	d -dim real space
L_d	Domain classifier loss	d^s, d^t	Source/target labels	\hat{y}_t	Target pseudo labels
γ_{mal}	Marginal alignment weight	N, M	Source/target sample size	\mathcal{H}	Hypothesis space
θ_d	Domain classifier parameters	∇_{θ_p}	Prompt gradient direction	θ_p	Prompt parameters
γ_{cal}	Conditional alignment weight	$f(x; \theta_p)$	Image encoder (e.g., CLIP)	T, I	Text/image features
$d_{\mathcal{H}}(P_s, P_t)$	Marginal distribution discrepancy	$d_{\mathcal{J}}(P_s, P_t)$	Total domain discrepancy	\mathbb{E}	Expectation (mean)
λ	Optimal joint error	$\epsilon_s(p), \epsilon_t(p)$	Source/target error	τ	Temperature coefficient
f_s, f_t	Source/target feature bank	I'	Augmented image features	P_{class}	Category prototypes
L_{cal}	Conditional alignment loss	$P_s(y_s I), P_t(\hat{y}_t I)$	Conditional distributions	$P_s(x), P_t(x)$	Marginal distributions

Table 1: Symbol Description

specific information. The work achieves this through a dynamically optimized adversarial training framework, formulated as a minimax game combined with a Gradient Reversal Layer (GRL).

Minimax Game Framework for Adversarial Training: Based on the image features I generated by the prompt, adversarial training aims to align the marginal distribution by maximizing the domain discriminator parameters θ_d and minimizing the prompt parameters θ_p . Specifically, the marginal alignment loss \mathcal{L}_{mal} is defined as:

$$\mathcal{L}_{\text{mal}} = \min_{\theta_p} \max_{\theta_d} \mathcal{L}_d = \min_{\theta_p} \max_{\theta_d} (\mathbb{E}_{x_s \sim P_s} [\log C_s(I_s)] + \mathbb{E}_{x_t \sim P_t} [\log(1 - C_t(I_t))]) \quad (7)$$

Here, the domain discriminator seeks to maximize θ_d to distinguish the origins of features (source vs. target), while the prompt aims to minimize θ_p to generate domain-invariant features that confuse the discriminator. This process balances the feature distribution, enabling the prompt-generated I to be domain-invariant. The domain discriminator loss \mathcal{L}_d is formulated as:

$$\mathcal{L}_d = -\frac{1}{N} \sum_{i=1}^N \log (P(d^s | I_i^s)) - \frac{1}{M} \sum_{j=1}^M \log (P(d^t | I_j^t)) \quad (8)$$

Where I_i^s and I_j^t denote the image features of the i -th and j -th samples from the source and target domains, respectively.

Gradient Reversal Layer (GRL) Mechanism: To minimize θ_p and facilitate adversarial training through gradient backpropagation, the work incorporates the Gradient Reversal Layer (GRL). During the forward pass, the GRL maintains an identity mapping. However, during the backward pass, it reverses the gradient of \mathcal{L}_d :

$$\frac{\partial \mathcal{L}_{\text{mal}}}{\partial \theta_p} \leftarrow -\frac{\partial \mathcal{L}_d}{\partial \theta_p} \quad (9)$$

Through gradient reversal, the GRL mechanism forces the prompt to generate semantically rich and domain-agnostic features, achieving marginal distribution alignment. This mechanism updates the prompt parameters as follows:

$$\theta_p \leftarrow \theta_p - \eta (\nabla_{\theta_p} L_{\text{cls}} + \gamma_{\text{mal}} \nabla_{\theta_p} L_{\text{mal}}) \quad (10)$$

This Dynamic Adversarial Alignment Framework ensures the prompt-generated features $I = f(x; \theta_p)$ possess Domain invariance feature ($P_s(I_s) \approx P_t(I_t)$) while retaining Semantic Richness for class discrimination, forming a solid foundation for the Conditional Distribution Alignment Branch.

Conditional Distribution Alignment Branch: Conditional Distribution Alignment via Class Mapping Mechanism

While marginal alignment is necessary, it is insufficient due to persistent conditional distribution discrepancies ($P_s(y_s | I_s) \neq P_t(\hat{y}_t | I_t)$), manifesting as class prototype shift (Tang et al., 2020). The Conditional Distribution Alignment Branch tackles this by explicitly aligning conditional distribution using the proposed Class Mapping Mechanism (CMM). CMM operates on the domain-invariant features I from the prompt. Assuming the source domain feature bank $f_s \in \mathbb{R}^d$ and the target domain feature bank $f_t \in \mathbb{R}^d$ are established as follows: The work proposes a CMM that maps image features I as the query ($Q = I$), f_s as the key, and f_t as the value ($K = f_s$ $V = f_t$), CMM enhance features through an attention mechanism to obtain $I' = \{I'_1, I'_2, \dots, I'_n\}$ and map I' to the target domain class prototypes:

$$I' = \text{softmax} \left(\frac{I f_s^T}{\sqrt{d}} \right) \cdot f_t + I \quad (11)$$

$$P_{\text{class}} = \text{Linear}(I') \quad (12)$$

I' furnishes a domain-invariant and semantically aligned feature basis for the prompt, reducing the complexity of learning cross-domain knowledge. The prompt is supervised by cross-entropy loss to constrain its understanding of class semantics. CMM effectively maps features to a domain-invariant class prototype space, standardizing semantic understanding across domains and mitigating source over-reliance. The conditional alignment loss \mathcal{L}_{cal} supervises this process, ensuring the mapped features I' accurately reflect the pseudo label distributions.

Synergistic Optimization and Inference

The core strength of C-DGPA lies in the synergistic optimization of its dual branches. Combined with the base clas-

Method	A→C	A→P	A→R	C→A	C→P	C→R	P→A	P→C	P→R	R→A	R→C	R→P	Avg
TVT	74.9	86.8	89.5	82.8	87.9	88.3	79.8	71.9	90.1	85.5	74.6	90.6	83.6
SDAT	69.1	86.6	88.9	81.9	86.2	88.0	81.0	66.7	89.7	86.2	72.1	91.9	82.4
SSRT	75.2	89.0	91.1	85.1	88.3	89.9	85.0	74.2	91.2	85.7	78.6	91.8	85.4
Deit-based	61.8	79.5	84.3	75.4	78.8	81.2	72.8	55.7	84.4	78.3	59.3	86.0	74.8
CDTrans-Deit	68.8	85.0	86.9	81.5	87.1	87.3	79.6	63.3	88.2	82.0	66.0	90.6	80.5
zero-shot CLIP	67.9	89.0	89.4	82.4	89.0	89.4	82.4	67.6	89.4	82.4	67.6	89.0	82.1
linear probe CLIP	60.1	73.7	80.9	66.4	76.4	76.8	63.4	61.0	82.3	74.7	64.8	88.3	72.4
CoOp	70.0	90.8	90.9	83.2	90.9	89.2	82.0	71.8	90.5	83.8	71.5	92.0	83.9
CoCoOp	70.4	91.4	90.4	83.5	91.8	90.3	83.4	67.0	91.0	83.4	71.2	91.7	84.1
VP	66.7	89.1	89.1	81.7	89.0	89.2	81.8	70.6	89.1	81.7	66.6	89.0	81.7
VPT-shallow	69.3	90.1	90.2	83.4	91.0	90.2	82.6	71.5	90.9	83.5	69.6	91.2	83.6
VPT-deep	71.6	89.9	90.3	82.8	91.0	89.7	82.0	72.4	90.3	84.6	71.7	91.6	83.9
IVLP	71.4	91.7	90.5	83.6	90.2	89.3	82.2	71.6	90.4	84.1	72.1	92.0	84.2
MaPLe	72.2	91.6	90.3	82.6	90.9	89.8	82.4	70.7	90.1	85.1	72.0	92.1	84.2
DAPL	70.7	91.0	90.9	85.2	91.0	91.0	85.1	70.7	90.9	85.3	70.4	91.4	84.4
PDA	73.5	91.4	91.3	86.0	91.6	91.5	86.0	73.5	91.7	86.4	73.0	92.4	85.7
C-DGPA (Ours)	74.7	91.3	91.6	87.2	91.5	91.4	86.9	75.6	91.9	87.6	75.3	93.2	86.5

Table 2: Comparisons with prompt-tuning methods and SOTA methods using ViT-B/16 as the backbone network on the Office-Home dataset. Bold indicates the best scores.

sification loss of CLIP \mathcal{L}_{cls} :

$$\mathcal{L}_{cls}^S = -\frac{1}{N} \sum_{i=1}^N y_i^s \log \frac{\exp(\langle T_i, I^s \rangle / \tau)}{\sum_k \exp(\langle T_k, I^s \rangle / \tau)} \quad (13)$$

$$\mathcal{L}_{cls}^T = -\frac{1}{M} \sum_{j=1}^M \hat{y}_j^t \log \frac{\exp(\langle T_j, I^t \rangle / \tau)}{\sum_k \exp(\langle T_k, I^t \rangle / \tau)} \quad (14)$$

$$\mathcal{L}_{cls} = \mathcal{L}_{cls}^S + \mathcal{L}_{cls}^T \quad (15)$$

The prompt parameters θ_p are updated end-to-end by minimizing the combined loss:

$$\mathcal{L} = \mathcal{L}_{cls} + \gamma_{cal} \mathcal{L}_{cal} + \gamma_{mal} \mathcal{L}_{mal} \quad (16)$$

where γ_{cal} and γ_{mal} are hyperparameters. The Marginal Distribution Alignment Branch provides domain-invariant features I , which are essential for the CMM in the Conditional Distribution Alignment Branch to effectively align class-specific distribution. Conversely, the improved class discriminability facilitated by CMM refines the feature space, benefiting the domain discriminator. This adaptive process progressively enhances both domain invariance and class separability. The prompt parameters are updated as follows:

$$\theta_p \leftarrow \theta_p - \eta (\nabla_{\theta_p} \mathcal{L}_{cls} + \gamma_{cal} \nabla_{\theta_p} \mathcal{L}_{cal} + \gamma_{mal} \nabla_{\theta_p} \mathcal{L}_{mal}) \quad (17)$$

Experiments

Experimental Setting

Datasets: Experiments were conducted on commonly used, high-quality unsupervised domain adaptation benchmark datasets, including Office31(Saenko et al. 2010), OfficeHome(Venkateswara et al. 2017), and VisDA-2017(Peng et al. 2018).

Baselines: The work compared C-DGPA with state-of-the-art UDA methods (both fine-tuning methods and SOTA methods). For comparisons using the ViT-B/16(Dosovitskiy et al. 2020) backbone, the models included TVT(Yang et al. 2023), SDAT(Rangwani et al. 2022), SSRT(Sun et al. 2022), Deit-based(Touvron et al. 2021), CDTrans-Deit(Xu et al. 2021), CLIP(Hu et al. 2024; Lai et al. 2024), CoOp(Zhou et al. 2022b), CoCoOp(Zhou et al. 2022a), VP(Bahng et al. 2022), VPT(Jia et al. 2022), IVLP(Khattak et al. 2023), MaPLe(Khattak et al. 2023), DAP(Ge et al. 2023), and PDA(Bai et al. 2024). For comparisons using the ResNet101(Dosovitskiy et al. 2020) backbone, the models included ERM, DANN(Ganin et al. 2016), MCD(Saito et al. 2018), MCC(Zhang et al. 2019), SDAT (Rangwani et al. 2022), and SHOT(Liang, Hu, and Feng 2020).

Experimental Setup: In terms of experimental configurations, the work selected ResNet101 and ViT-B/16 as the backbone networks. For ResNet-based backbones, text prompts were used for prompt design, while multimodal prompts were employed for ViT-based backbones. The parameters in the CLIP encoder were kept fixed. The work used the SGD optimizer to train the prompts for 10 epochs on the VisDA-2017 dataset and 30 epochs on the Office31 and OfficeHome datasets, with a batch size of 32. The initial learning rate was set to 0.003 and was decreased according to the cosine annealing schedule. Additionally, the context length for C-DGPA was set to 16.

Comparisons on the OfficeHome Dataset

As shown in Table 2, C-DGPA achieves an average accuracy of 86.5% on the OfficeHome dataset, surpassing all comparison methods. This represents a significant improvement of 4.4% compared to zero-shot CLIP (82.1%). Specifically, in the subtask "Real-World to Clipart" (R→C), C-DGPA attains an accuracy of 75.3%, outperforming PDA (73.0%), MaPLe (72.0%), and VPT-deep (71.7%) by 2.3%, 3.3%, and 3.6%, respectively. Additionally, in tasks with larger cross-

Backbone	Method	plane	bicycle	bus	car	horse	knife	mcycl	person	plant	sktbrd	train	truck	Avg
ResNet101	ERM	55.1	53.3	61.9	59.1	80.6	17.9	79.7	31.2	81.0	26.5	73.5	8.5	52.4
	DANN	81.9	77.7	82.8	44.3	81.2	29.5	65.1	28.6	51.9	54.6	82.8	7.8	57.4
	SDAT	94.8	77.1	82.8	60.9	92.3	95.2	91.7	79.9	89.9	91.2	88.5	41.2	82.1
	MCC	88.1	80.3	80.5	71.5	90.1	93.2	85.0	71.6	89.4	73.8	85.0	36.9	78.8
	MCD	87.0	60.9	83.7	64.0	88.9	79.6	84.7	76.9	88.6	40.3	83.0	25.8	71.9
	SHOT	94.3	88.5	80.1	57.3	93.1	94.9	80.7	80.3	91.5	89.1	86.3	58.2	82.9
	C-DGPA (Ours)	98.2	84.5	91.4	72.6	97.5	93.3	94.3	79.3	86.8	86.1	91.1	63.5	86.6
ViT-B/16	CLIP	99.2	92.2	93.5	76.7	98.3	90.4	94.6	83.6	85.4	96.1	94.3	62.7	88.9
	VPT	98.7	78.2	96.0	72.8	98.8	70.5	98.2	82.5	87.4	93.1	94.3	54.6	85.4
	CoOp	98.7	88.8	87.2	69.7	99.0	71.5	96.3	53.9	91.5	96.3	95.8	35.7	82.0
	CoCoOp	99.1	92.4	92.0	71.7	99.1	73.4	95.8	44.5	90.3	95.6	96.0	52.8	83.6
	IVLP	98.2	71.2	82.6	79.9	97.3	68.3	98.2	59.0	90.5	93.4	95.7	36.6	80.9
	MaPLe	98.4	83.4	88.8	67.8	98.8	75.2	95.7	77.7	81.7	95.4	95.6	40.4	83.2
	DAPL	98.9	92.6	93.1	77.7	98.6	91.1	94.4	83.5	87.5	95.9	93.7	63.7	89.2
C-DGPA (Ours)	PDA	99.2	91.1	91.9	77.1	98.4	93.6	95.1	84.9	87.2	97.3	95.3	65.3	89.7
	C-DGPA (Ours)	99.2	94.3	94.0	77.6	99.2	94.3	94.4	85.6	88.8	95.4	94.8	65.1	90.2

Table 3: Comparisons with prompt-tuning methods and SOTA methods using ViT-B/16 and ResNet101 as backbone networks on the VisDA-17 dataset. Bold indicates the best scores.

domain differences, such as "Product to Clipart" (P→C), C-DGPA demonstrates particularly strong performance, with accuracy leading SDAT and SSRT by 8.9% and 1.4%, respectively. Notably, IVLP and DAPL, which are based on multimodal prompts, lag behind C-DGPA by 2.3% and 2.1% in average performance on the OfficeHome dataset, further validating the effectiveness of aligning both marginal and conditional distribution simultaneously.

Comparisons on the VisDA-2017 Dataset

As shown in Table 3, on the VisDA-2017 dataset, C-DGPA establishes a new state-of-the-art by obtaining 90.2 % accuracy with the ViT-B/16 backbone, surpassing prompt-tuning leaders PDA (89.7 %), DAPL (89.2 %), MaPLe (83.2 %) and CoOp (82.0 %) by clear margins of 0.5–8.2 percentage points , while with ResNet101 it reaches 86.6 %, comfortably exceeding MCD (71.9 %), MCC (78.8 %) and even SDAT (82.1 %); notably, SHOT—also built on ResNet101—stops at 82.9 %, further attesting that C-DGPA's dual alignment of marginal and conditional distributions delivers robust, architecture-agnostic gains.

Comparisons on the Office31 Dataset

As shown in Table 4, C-DGPA achieved the best performance on the Office31 dataset, with an average accuracy of 91.8%, representing a significant improvement of 14.3% over zero-shot CLIP. In most tasks, C-DGPA outperformed other methods. For example, in the A→D task, C-DGPA's accuracy exceeded that of PDA, MaPLe, and VPT-deep by 2.4%, 6.7%, and 4.0%, respectively. C-DGPA also achieved the best performance in the A→W, D→W, and W→D tasks. Additionally, The work noted that although CoCoOp is built upon CoOp, its average performance on the Office31 dataset was 0.5% lower than that of CoOp.

Ablation Study

Ablation Study on Dual-Branch Alignment Strategy:

Table 5 demonstrates that combining \mathcal{L}_{mal} and \mathcal{L}_{cal}

Method	A-D	A-W	D-A	D-W	W-A	W-D	Avg
zero-shot CLIP	77.7	75.8	79.0	75.8	79.0	77.7	77.5
linear probe CLIP	83.1	83.3	74.2	96.5	70.3	98.4	84.3
CoOp	88.5	88.5	82.0	96.1	82.4	99.0	89.4
CoCoOp	86.9	88.2	83.2	94.1	82.8	98.0	88.9
VP	78.5	74.8	77.9	77.5	77.8	79.7	77.4
VPT-shallow	83.5	83.8	77.5	88.6	80.9	91.2	84.2
VPT-deep	89.6	86.5	81.9	96.5	82.8	99.2	89.4
IVLP	85.7	89.2	81.9	98.4	80.3	99.2	89.1
MaPLe	86.9	88.6	83.0	97.7	82.0	99.4	89.6
DAPL	81.7	80.3	81.2	81.8	81.0	81.3	81.2
PDA	91.2	92.1	83.5	98.1	82.5	99.8	91.2
C-DGPA (Ours)	93.6	93.7	82.6	98.6	82.4	99.8	91.8

Table 4: Comparison of prompt-tuning methods using ViT-B/16 as the backbone network on the Office31 dataset. Bold indicates the best scores.

yields optimal performance: Office31/ViT (91.8%), Office-Home/ViT (86.5%), VisDA-2017/ViT (90.2%), and VisDA-2017/Res (86.6%). Using only \mathcal{L}_{mal} slightly reduces accuracy (e.g., -0.3% on OfficeHome/ViT), while \mathcal{L}_{cal} alone leads to a larger drop (-0.8%). On VisDA-2017, dual-loss optimization provides stable gains (+0.2–0.3%), confirming their complementary effect. The same trend holds for ResNet, proving architecture-agnostic universality.

\mathcal{L}_{mal}	\mathcal{L}_{cal}	Office31/ViT	OfficeHome/ViT	Visda2017/ViT	Visda2017/Res
✓	✓	91.8	86.5	90.2	86.6
✗	✓	91.3	86.2	90.0	86.4
✓	✗	91.1	85.7	89.9	86.1

Table 5: The impact of different branches (Marginal + Conditional) on domain adaptation.

Analysis of Key Hyperparameters

Analysis Weight Of Marginal And Conditional Alignment Loss: As shown in Table 6, the hyperparameter study reveals critical tradeoffs for marginal alignment loss weight (γ_{mal}) and conditional alignment loss weight (γ_{cal}). An optimal $\gamma_{mal} = 0.01$ maximizes average accuracy (86.5% on OfficeHome), with strong performance in both A domain (87.2%) and P domain (92.0%). However, excessive marginal alignment weighting ($\gamma_{mal} = 2$) over-suppresses domain-specific features, reducing discriminability and causing a 0.8% average accuracy drop (85.7%). For conditional alignment, $\gamma_{cal} = 1$ achieves the best equilibrium (C domain: 75.2%), while increasing to $\gamma_{cal} = 2$ boosts P domain accuracy to 92.0% but destabilizes other domains. Conversely, reducing to $\gamma_{cal} = 0.1$ weakens class alignment, lowering C domain accuracy by 1.1%.

γ_{mal}	A	C	P	R	Avg
2	86.6	73.8	91.2	91.1	85.7
1	86.7	73.8	91.1	91.2	85.7
0.1	87.0	74.7	91.8	91.6	86.3
0.01	87.2	75.2	92.0	91.6	86.5

γ_{cal}	A	C	P	R	Avg
2	86.9	74.2	92.0	91.7	86.2
1	87.2	75.2	92.0	91.6	86.5
0.1	87.2	74.1	91.8	91.4	86.1
0.01	86.0	73.4	91.6	91.2	85.6

(a) The impact of γ_{mal} on OfficeHome.

(b) The impact of γ_{cal} on OfficeHome.

Table 6: Performance comparison under different γ settings

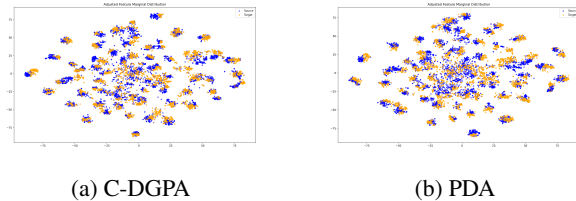


Figure 2: t-SNE visualization of source and target domain features, highlighting marginal distribution using C-DGPA and PDA (OfficeHome dataset, R→P).

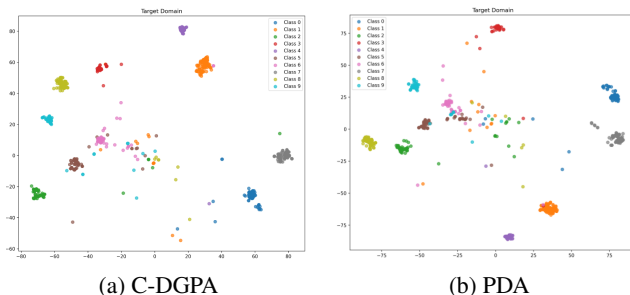


Figure 3: t-SNE visualization of target domain features, highlighting conditional distribution using C-DGPA and PDA (OfficeHome dataset, R→P).

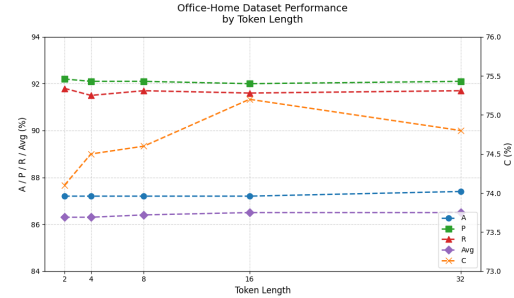


Figure 4: The impact of different token lengths on accuracy (OfficeHome dataset)

Visualization Analysis

The t-SNE visualization (Figure 2) shows that PDA (only marginal alignment) results in partial domain overlap but significant same-class center offset. Target domain features are dispersed with blurred boundaries, indicating poor conditional distribution alignment. In contrast (Figure 3), C-DGPA (joint marginal + conditional alignment) produces highly overlapping target features with compact intra-class structure and clear inter-class boundaries. This demonstrates the effectiveness of joint alignment in mitigating class prototype shift.

The Impact of Token Length on Accuracy: Figure 4 shows token length's impact on OfficeHome accuracy. Accuracy peaks at 86.5% with 16 tokens, rising initially before stabilizing. Shorter tokens (≤ 4) limit semantic capacity, reducing C domain performance (74.1%-74.5%). Longer tokens (≥ 16) marginally improve A domain accuracy (87.4%) but increase computational costs with diminishing returns. A length of 16 optimally balances semantic expression and efficiency.

Conclusion

The work introduces C-DGPA, a class-centric dual-alignment framework that adapts vision-language models to unsupervised domain adaptation by tackling the critical limitation of prior prompt-tuning methods: their exclusive focus on marginal distribution. C-DGPA resolves the joint discrepancy—both marginal and conditional—via a synergistic two-branch architecture, yielding new state-of-the-art results on OfficeHome, Office31 and VisDA-2017. The marginal branch employs a dynamic adversarial minimax game with gradient reversal to align cross-domain feature marginals, while the conditional branch leverages a Class Mapping Mechanism that aligns class prototypes and mitigates semantic drift. Jointly optimized, the branches reciprocally enhance domain invariance and class discrimination. Future work will focus on extending C-DGPA to more complex scenarios, such as source-free domain adaptation, multi-target domain adaptation, and domain generalization, to further improve its applicability and effectiveness in a broader range of tasks.

Acknowledgments

To maintain anonymity, this section will remain blank for now. If it passes the review, We will provide the necessary additions later.

References

Bahng, H.; Jahanian, A.; Sankaranarayanan, S.; and Isola, P. 2022. Exploring visual prompts for adapting large-scale models. *arXiv preprint arXiv:2203.17274*.

Bai, S.; Zhang, M.; Zhou, W.; Huang, S.; Luan, Z.; Wang, D.; and Chen, B. 2024. Prompt-based distribution alignment for unsupervised domain adaptation. In *Proceedings of the AAAI conference on artificial intelligence*, volume 38, 729–737.

Ben-David, S.; Blitzer, J.; Crammer, K.; Kulesza, A.; Pereira, F.; and Vaughan, J. W. 2010. A theory of learning from different domains. *Machine learning*, 79: 151–175.

Dosovitskiy, A.; Beyer, L.; Kolesnikov, A.; Weissenborn, D.; Zhai, X.; Unterthiner, T.; Dehghani, M.; Minderer, M.; Heigold, G.; Gelly, S.; et al. 2020. An image is worth 16x16 words: Transformers for image recognition at scale. *arXiv preprint arXiv:2010.11929*.

Ganin, Y.; and Lempitsky, V. 2015. Unsupervised domain adaptation by backpropagation. In *International conference on machine learning*, 1180–1189. PMLR.

Ganin, Y.; Ustinova, E.; Ajakan, H.; Germain, P.; Larochelle, H.; Laviolette, F.; March, M.; and Lempitsky, V. 2016. Domain-adversarial training of neural networks. *Journal of machine learning research*, 17(59): 1–35.

Ge, C.; Huang, R.; Xie, M.; Lai, Z.; Song, S.; Li, S.; and Huang, G. 2023. Domain adaptation via prompt learning. *IEEE Transactions on Neural Networks and Learning Systems*.

Gu, Y.; Han, X.; Liu, Z.; and Huang, M. 2021. Ppt: Pre-trained prompt tuning for few-shot learning. *arXiv preprint arXiv:2109.04332*.

Hu, X.; Zhang, K.; Xia, L.; Chen, A.; Luo, J.; Sun, Y.; Wang, K.; Qiao, N.; Zeng, X.; Sun, M.; et al. 2024. Reclip: Refine contrastive language image pre-training with source free domain adaptation. In *Proceedings of the IEEE/CVF Winter Conference on Applications of Computer Vision*, 2994–3003.

Jia, M.; Tang, L.; Chen, B.-C.; Cardie, C.; Belongie, S.; Hariharan, B.; and Lim, S.-N. 2022. Visual prompt tuning. In *European conference on computer vision*, 709–727. Springer.

Khattak, M. U.; Rasheed, H.; Maaz, M.; Khan, S.; and Khan, F. S. 2023. Maple: Multi-modal prompt learning. In *Proceedings of the IEEE/CVF conference on computer vision and pattern recognition*, 19113–19122.

Lai, Z.; Bai, H.; Zhang, H.; Du, X.; Shan, J.; Yang, Y.; Chuah, C.-N.; and Cao, M. 2024. Empowering unsupervised domain adaptation with large-scale pre-trained vision-language models. In *Proceedings of the ieee/cvf winter conference on applications of computer vision*, 2691–2701.

Lai, Z.; Vesdapunt, N.; Zhou, N.; Wu, J.; Huynh, C. P.; Li, X.; Fu, K. K.; and Chuah, C.-N. 2023. Padclip: Pseudo-labeling with adaptive debiasing in clip for unsupervised domain adaptation. In *Proceedings of the IEEE/CVF International Conference on Computer Vision*, 16155–16165.

Liang, J.; Hu, D.; and Feng, J. 2020. Do we really need to access the source data? source hypothesis transfer for unsupervised domain adaptation. In *International conference on machine learning*, 6028–6039. PMLR.

Litrico, M.; Del Bue, A.; and Morerio, P. 2023. Guiding pseudo-labels with uncertainty estimation for source-free unsupervised domain adaptation. In *Proceedings of the IEEE/CVF Conference on Computer Vision and Pattern Recognition*, 7640–7650.

Long, M.; Cao, Y.; Wang, J.; and Jordan, M. 2015. Learning transferable features with deep adaptation networks. In *International conference on machine learning*, 97–105. PMLR.

Peng, X.; Usman, B.; Kaushik, N.; Wang, D.; Hoffman, J.; and Saenko, K. 2018. Visda: A synthetic-to-real benchmark for visual domain adaptation. In *Proceedings of the IEEE Conference on Computer Vision and Pattern Recognition Workshops*, 2021–2026.

Pfeiffer, J.; Ruder, S.; Vulic, I.; and Ponti, E. M. 2023. Modular deep learning. *arXiv preprint arXiv:2302.11529*.

Radford, A.; Kim, J. W.; Hallacy, C.; Ramesh, A.; Goh, G.; Agarwal, S.; Sastry, G.; Askell, A.; Mishkin, P.; Clark, J.; et al. 2021. Learning transferable visual models from natural language supervision. In *International conference on machine learning*, 8748–8763. PMLR.

Rangwani, H.; Aithal, S. K.; Mishra, M.; Jain, A.; and Radhakrishnan, V. B. 2022. A closer look at smoothness in domain adversarial training. In *International conference on machine learning*, 18378–18399. PMLR.

Reynolds, L.; and McDonell, K. 2021. Prompt programming for large language models: Beyond the few-shot paradigm. In *Extended abstracts of the 2021 CHI conference on human factors in computing systems*, 1–7.

Saenko, K.; Kulis, B.; Fritz, M.; and Darrell, T. 2010. Adapting visual category models to new domains. In *Computer vision–ECCV 2010: 11th European conference on computer vision, Heraklion, Crete, Greece, September 5–11, 2010, proceedings, part iV 11*, 213–226. Springer.

Saito, K.; Watanabe, K.; Ushiku, Y.; and Harada, T. 2018. Maximum classifier discrepancy for unsupervised domain adaptation. In *Proceedings of the IEEE conference on computer vision and pattern recognition*, 3723–3732.

Sun, T.; Lu, C.; Zhang, T.; and Ling, H. 2022. Safe self-refinement for transformer-based domain adaptation. In *Proceedings of the IEEE/CVF conference on computer vision and pattern recognition*, 7191–7200.

Tang, H.; Chen, K.; and Jia, K. 2020. Unsupervised domain adaptation via structurally regularized deep clustering. In *Proceedings of the IEEE/CVF conference on computer vision and pattern recognition*, 8725–8735.

Touvron, H.; Cord, M.; Douze, M.; Massa, F.; Sablayrolles, A.; and Jégou, H. 2021. Training data-efficient image transformers & distillation through attention. In *International conference on machine learning*, 10347–10357. PMLR.

Venkateswara, H.; Eusebio, J.; Chakraborty, S.; and Panchanathan, S. 2017. Deep hashing network for unsupervised domain adaptation. In *Proceedings of the IEEE conference on computer vision and pattern recognition*, 5018–5027.

Wilson, G.; and Cook, D. J. 2020. A survey of unsupervised deep domain adaptation. *ACM Transactions on Intelligent Systems and Technology (TIST)*, 11(5): 1–46.

Xu, T.; Chen, W.; Wang, P.; Wang, F.; Li, H.; and Jin, R. 2021. Cdtrans: Cross-domain transformer for unsupervised domain adaptation. *arXiv preprint arXiv:2109.06165*.

Yang, J.; Liu, J.; Xu, N.; and Huang, J. 2023. Tvt: Transferable vision transformer for unsupervised domain adaptation. In *Proceedings of the IEEE/CVF winter conference on applications of computer vision*, 520–530.

Zhang, M.; Huang, S.; and Wang, D. 2022. Domain generalized few-shot image classification via meta regularization network. In *ICASSP 2022-2022 IEEE International Conference on Acoustics, Speech and Signal Processing (ICASSP)*, 3748–3752. IEEE.

Zhang, M.; Wang, D.; and Gai, S. 2020. Knowledge distillation for model-agnostic meta-learning. In *ECAI 2020*, 1355–1362. IOS Press.

Zhang, Y.; Liu, T.; Long, M.; and Jordan, M. 2019. Bridging theory and algorithm for domain adaptation. In *International conference on machine learning*, 7404–7413. PMLR.

Zhou, K.; Yang, J.; Loy, C. C.; and Liu, Z. 2022a. Conditional prompt learning for vision-language models. In *Proceedings of the IEEE/CVF conference on computer vision and pattern recognition*, 16816–16825.

Zhou, K.; Yang, J.; Loy, C. C.; and Liu, Z. 2022b. Learning to prompt for vision-language models. *International Journal of Computer Vision*, 130(9): 2337–2348.

Zhu, D.; Li, Y.; Shao, Y.; Hao, J.; Wu, F.; Kuang, K.; Xiao, J.; and Wu, C. 2023a. Generalized universal domain adaptation with generative flow networks. In *Proceedings of the 31st ACM International Conference on Multimedia*, 8304–8315.

Zhu, D.; Li, Y.; Zhang, M.; Yuan, J.; Liu, J.; Kuang, K.; and Wu, C. 2023b. Bridging the gap: neural collapse inspired prompt tuning for generalization under class imbalance. *arXiv preprint arXiv:2306.15955*.